Diffusion of Aromatic Molecules in Zeolite NaY. 2. Dynamical Corrections

Thomas Mosell,[†] Gerhard Schrimpf,[†,‡] and Jürgen Brickmann*[,†,§]

Physical Chemistry I and Darmstadt Center for Scientific Computing (DZWR), Darmstadt University of Technology, Petersenstrasse 20, D-64287 Darmstadt, Germany

Received: April 16, 1997; In Final Form: August 4, 1997[⊗]

Molecular dynamics simulations of individual trajectories that are started in the transition state for cage-to-cage diffusion are presented for benzene and *p*-xylene in zeolite NaY. Furthermore, diffusion coefficients and the activation energies for the diffusion are determined from a hopping model that considers dynamical corrections. The transmission coefficients for both molecules are small, particularly at low temperatures. The influence of the window adsorption site of benzene on the transmission coefficient is investigated. The hopping model fails for the treatment of the diffusion of benzene at high temperatures $T > 700$ K, because the diffusion cannot be divided into different jump events at such temperatures. The results for the diffusion coefficient of *p*-xylene are in very good agreement with experimental results, whereas for benzene an activation energy results that is slightly too high. This fact is related to the possibility of a dependence of the activation energy on the exact positions of the sodium ions.

I. Introduction

Experiments on the diffusion of aromatic molecules in zeolites NaX and NaY have lead to partially contradictory results. Activation energies between 22.5 and 25 kJ/mol have repeatedly been measured for the diffusion of benzene in zeolite NaX,[1−4] but activation energies of 14 and 34 kJ/mol, depending on the loading, have also been reported for this system.[5] The results for benzene in zeolite NaY are even more inconsistent. Bull et al.[6] and Sousa Gonçalves et al.[7] determined activation energies of 23.5 and 25.8 kJ/mol, respectively, by ^{2}H NMR, whereas Burmeister et al.[8] obtained an activation energy of 13.7 kJ/mol with the same technique. Forni and Viscardi[9] determined an activation energy of 46 kJ/mol by a gas chromatographic pulse method. Lechert and Wittern[5] found activation energies of 18 and 38 kJ/mol at different loadings. However, the different results for the activation energy of benzene in zeolite NaY cannot solely be explained by a dependence of the activation energy on the loading.

The diffusion of *p*-xylene in zeolites NaX and NaY has been investigated less frequently. The experimental results for the diffusion coefficient of *p*-xylene[1,2,7,10,11] are smaller than those for benzene in these zeolites. Goddard and co-workers[2,10,11] determined an activation energy of 26 kJ/mol for *p*-xylene in zeolite NaX by different experimental techniques. Germanus et al.[1] not only found activation energies between 20 kJ/mol at high and 25 kJ/mol at low loadings for this system by PFG (pulsed field gradient) NMR but also reported an increase of the activation energy when the Si/Al ratio is increased. In accordance with the latter result, an activation energy of 32 kJ/mol was determined by Sousa Gonçalves et al.[7] for cage-to-cage jumps of *p*-xylene in zeolite NaY.

Different measurements of the diffusion coefficient of an aromatic guest molecule result in discrepancies of up to 3 orders of magnitude at the same temperature.[12] Although Goddard and co-workers[2,10,11] determined the same diffusion coefficient by microscopic and macroscopic methods, measurements on a microscopic level usually tend to give larger diffusion coefficients than those on a macroscopic scale. Garcia and Weisz[13] suggested that only the molecules that actually migrate are observed in NMR experiments on a microscopic scale, while most of the molecules are not recorded with this technique. On the other hand, Joly and Tessa[14] attributed the discrepancies to the influence of heat transfer in the macroscopic measurements. A variety of other possible reasons have been discussed as well.[12] In summary, different aspects of the diffusion of aromatic molecules in zeolites NaX and NaY have not been fully explained so far.

Conventional molecular dynamics (MD) simulations are only of limited suitability for investigations into these diffusion processes, because jumps between adsorption sites are rare events on the time scale of MD simulations in the temperature range of interest.[6] The theoretical investigation of these systems should therefore be based on a hopping model. Auerbach et al.[15] investigated the diffusion of benzene in zeolite NaY with a Monte Carlo based approach and determined an activation energy of 41 kJ/mol for the diffusion process. However, the jump probabilities in that study were based simply on the minimum-energy difference between the configuration at the adsorption site and in their transition state. In a study on the diffusion of guest molecules in silicalite, June et al.[16] not only determined their jump rates from the whole configurational space but also considered dynamical corrections to the jump rates.

We have presented a hopping model for the diffusion in zeolite NaY at infinite dilution and applied it to the diffusion of xenon in zeolite NaY at very low temperatures.[17,18] This hopping model considers jumps between different supercages only. The jump rate is obtained from the probability density for a transition-state plane that is parallel to the window plane between two supercages. In the hopping model, the transmission coefficient for the transition-state plane and the different lengths of the jump events are taken into account as dynamical corrections.

In a previous publication (hereafter referred to as paper I),[19] we applied constrained reaction coordinate dynamics (CRCD)[20] to benzene and *p*-xylene in zeolite NaY in order to determine the potential of mean force along a reaction coordinate that is

* To whom correspondence should be addressed.
† Physical Chemistry I.
‡ Present address: IBM Deutschland, Information Systems, P.O. Box 103068, D-69020 Heidelberg, Germany.
§ DZWR.
⊗ Abstract published in *Advance ACS Abstracts,* November 1, 1997.

S1089-5647(97)01327-8 CCC: $14.00

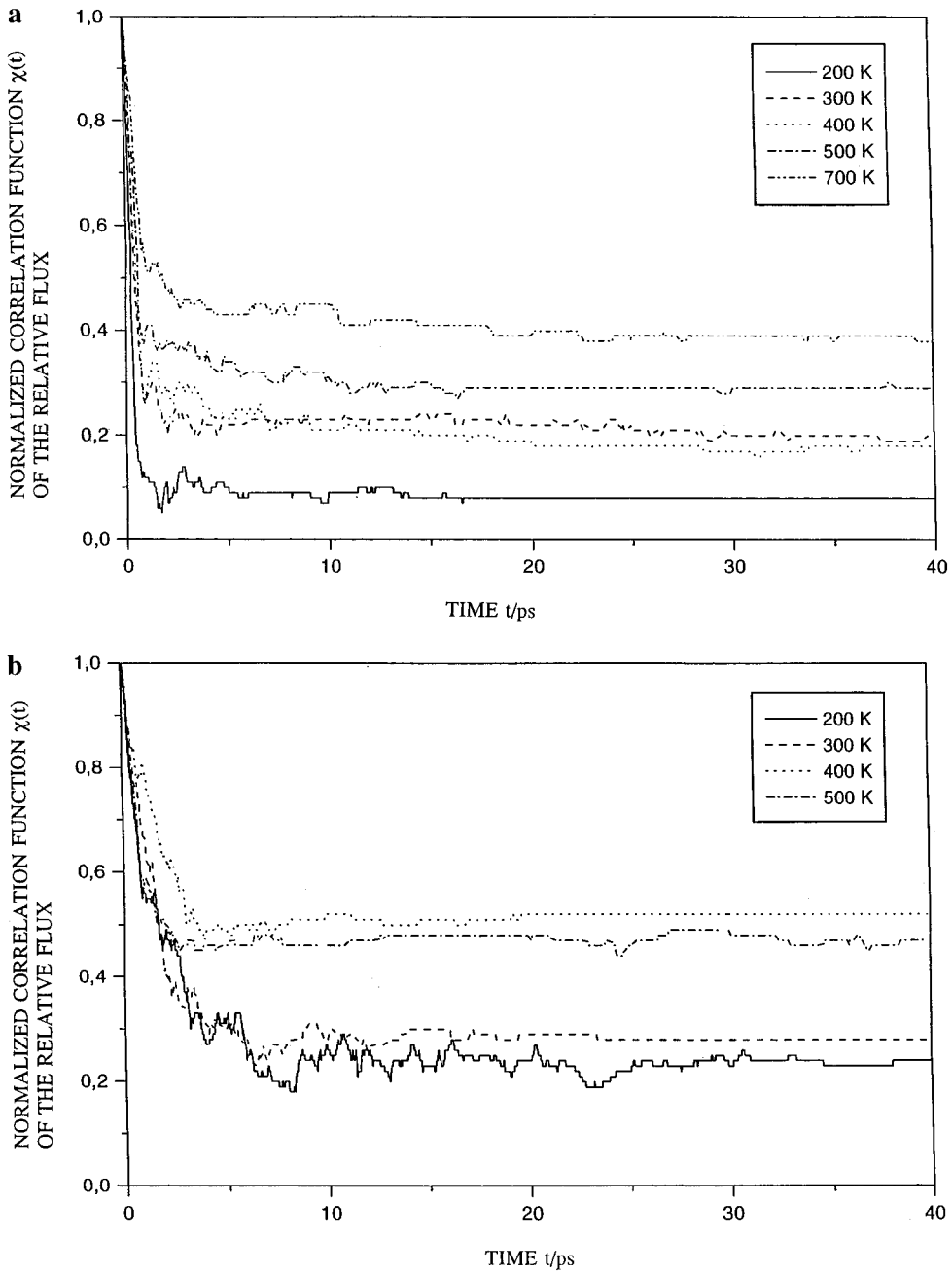

Figure 1. Normalized reactive-flux correlation function $\kappa(t)$ for the transition-state planes of benzene (a) and *p*-xylene (b) in zeolite NaY at different temperatures.

perpendicular to the window. The transition-state theory values of the jump rate were calculated from the potential of mean force. In this work, the dynamical corrections are determined from MD simulations which are started in the transition-state plane. Subsequently, the results at different temperatures are used to calculate the diffusion coefficients and the activation energy for the diffusion process by the hopping model of ref 18.

This paper is divided as follows. The model system is described in section II. Section III is concerned with the methods used in this work. Some details about the calculations are presented in section IV. In section V, the results of the MD simulations are reported. Section VI contains the results of the hopping model calculations. The conclusions are stated in section VII.

II. Model System

The model system for benzene and *p*-xylene in zeolite NaY is the same as in paper I.[19] The aromatic molecules are treated as rigid bodies, and the methyl groups of *p*-xylene are described as united atoms. The Lennard-Jones and Coulomb interactions between the aromatic molecules and the zeolite are based on a force field of Demontis et al.[21] The Lennard-Jones parameters for the methyl group were taken from Bezus et al.,[22] and the partial charges for *p*-xylene were adapted from the results of AM1[23] calculations. For the interactions between the zeolite atoms, the valence force field of Schrimpf et al.[24] was used, describing Si and Al atoms by a joint atom type T. This force field uses bonded potentials for the interactions between sodium and oxygen, excluding the possibility for a diffusion of sodium ions. The parameters for the zeolite−zeolite interactions and the interactions between the zeolite and the guest molecule were listed explicitly in refs 24 and 19, respectively.

The experimental sodium positions in zeolite NaX and NaY are depicted in Figure 1 of paper I. Fitch et al.[25] investigated the structure of zeolite NaY and found that position S_{II}, which is located inside the supercage in front of the 6-T-ring of the sodalite cage, is occupied completely, whereas positions S_I and

$S_{I'}$, which are located outside the supercage, are both partially occupied. At higher aluminum content, e.g. in zeolite NaX, position S_{III} is occupied as well.[3] In the model of zeolite NaY used in this work, the number of sodium ions corresponds to a Si/Al ratio of 3:1. The $S_{I'}$ position is not considered explicitly, because it is in the vicinity of position S_I and cannot be reached by the guest molecules. Only the positions S_I and S_{II}, both fully occupied, are considered.

III. Method

A. Transmission Coefficients. Wigner[26] showed that transition-state theory[27] is equal to the assumption that no recrossings occur after a trajectory has passed the transition state. The deviations of a rate constant (or jump rate) k from its transition-state theory value can therefore be described by a transmission coefficient κ:

$$k = \kappa/k^{\mathrm{TST}} \tag{1}$$

This transmission coefficient κ is obtained from MD simulations of many independent trajectories that are started in the transition state. From these trajectories, the reactive-flux correlation function can be determined.[28] The normalized reactive-flux correlation function $\kappa(t)$ is calculated from[29,30]

$$\kappa(t) = \frac{\langle \dot{r}(0)\, \delta(r(0) - r^{\ddagger})\, \theta(r(t) - r^{\ddagger})\rangle}{\langle \dot{r}(0)\, \delta(r(0) - r^{\ddagger})\, \theta(\dot{r}(0))\rangle} \tag{2}$$

where $r(t)$ is the position on the reaction coordinate, $r^{\ddagger}$ the location of the transition state, δ the Dirac delta function, and θ the Heavyside function:

$$\theta(r^{\ddagger} - r(t)) = \begin{cases} 1 & r^{\ddagger} \geq r(t) \\ 0 & r^{\ddagger} < r(t) \end{cases} \tag{3}$$

If the activation barrier is at least a few $k_B T$, the normalized reactive-flux correlation function $\kappa(t)$ will display a plateau. After the initial decrease due to trajectories that recross the transition state during the same rare event, only the part of the flux that has resulted in the formation of products contributes to the reactive flux. Thus, the plateau value of the normalized reactive flux must be equal to the transmission coefficient.[29,30]

The velocity component $\dot{r}(0)$ along the reaction coordinate in both the numerator and denominator of eq 2 indicates that flux-weighted averaging has to be carried out. This was taken into account by choosing the starting configurations from a flux-weighted distribution. As a result, $\kappa(t)$ is obtained from a sum over all trajectories:[31]

$$\kappa(t) = \frac{1}{N_+}\sum_{i=1}^{N_+}\theta(r(t) - r^{\ddagger}) - \frac{1}{N_-}\sum_{i=1}^{N_-}\theta(r^{\ddagger} - r(t)) \tag{4}$$

where $\kappa(t)$ has been divided into the contributions that arise from N_+ trajectories with a positive and N_- trajectories with a negative velocity component in the transition state.

B. Hopping Model. The hopping model[18] can be used to calculate the diffusion coefficient at inifinite dilution. Only jumps between adsorption sites in different supercages are considered. As a result, the diffusion is simplified to the diffusion process on the lattice formed by the centers of the supercages. This lattice is a diamond lattice. A jump event consists of the adsorption-site changes during one rare event and may contain several successive barrier passages. The probability γ for the continuation of a jump event is assumed to be independent of the previous number of barrier passages within the jump event. Furthermore, it is assumed that the guest molecules leave the supercage through each of the windows with the same probability.

The hopping model takes two different dynamical corrections into account. Besides the transmission coefficient κ, an absorbing-boundary factor[17] χ is used to take into account the jump events with several barrier passages. An absorbing boundary is placed in all the windows that surround the two supercages located on either side of the central window region. The absorbing-boundary function $\chi(t)$ is defined as the part of the trajectories that has been "absorbed" at the boundaries of the two-supercage region. Just as the normalized reactive-flux correlation function $\kappa(t)$, the absorbing-boundary function $\chi(t)$ will display a plateau, if the activation barrier is high enough. The absorbing-boundary factor χ is defined by this plateau value of $\chi(t)$.

However, the determination of κ and χ may be possible, although $\kappa(t)$ and $\chi(t)$ do not exhibit a true plateau after the end of the initial jump events. The occurrence of new rare events may lead to a slow decrease of the normalized reactive-flux correlation function $\kappa(t)$ or to a slow increase of the absorbing-boundary function $\chi(t)$. In this case, the transmission coefficient κ may be obtained by linearly extrapolating $\kappa(t)$ to $t = 0$.[32] We apply the same procedure to obtain the absorbing-boundary factor χ from $\chi(t)$.[17] Note, however, that there will be no plateaulike behavior if it is impossible to divide the diffusion process into separate jump events, because there is no separation between the time scale of recrossings during the same jump event and the time scale of independent jump events.

Due to the consideration of the dynamic corrections, the standard expression for the diffusion coefficient D on the diamond lattice[33]

$$D = {}^1/_8 \Gamma_0 a^2 \tag{5}$$

as a function of the number of individual jumps Γ_0 (corresponding to k^{TST}) and the length a of the unit cell is modified to[18]

$$D = {}^1/_8 \kappa' n_{\mathrm{BP}} k^{\mathrm{TST}} a^2 \tag{6}$$

where n_{BP} is the mean number of barrier passages per jump event and κ' is a local transmission coefficient which is connected with the recrossings during a single barrier passage within the jump event.

Under the conditions of our hopping model, the mean number n_{BP} of barrier passages per jump event can be expressed in terms of the probability γ of the continuation of the jump event:

$$n_{\mathrm{BP}} = \frac{1}{1 - \gamma} \tag{7}$$

and the local transmission coefficient κ' is linked to the transmission coefficient κ obtained from the MD simulations by

$$\kappa' = \kappa + \frac{\gamma}{4 + \gamma} \tag{8}$$

The probabability γ of the continuation of the jump event is given by

$$\gamma = 2\frac{\sqrt{(3 - \chi)^2 + 4\kappa\chi(3 + (1 + \kappa)\chi)} - (3 - \chi)}{3 + (1 + \kappa)\chi} \tag{9}$$

so that the diffusion coefficient in eq 6 can be calculated from

TABLE 1: Transmission Coefficient for Cage-to-Cage Diffusion of Benzene and *p*-Xylene in Zeolite NaY

	transmission coefficient κ	
temperature T [K]	benzene	*p*-xylene
200	0.08	0.24
300	0.20	0.28
400	0.18	0.52
500	0.29	0.47
700	0.39	*a*

[a] No simulations at this temperature.

the transition-state value for the number of jump events k^{TST}, the transmission coefficient κ, and the absorbing-boundary factor χ.

IV. Details of the Calculations

The trajectories were started from the transition state defined in paper I.[19] The reaction coordinate d is chosen to be parallel to the body diagonal [1 1 1] of the unit cell. The reaction coordinate is defined by the distance between the center of mass of the aromatic molecule and the window plane at the boundary between two supercages. The transition states for benzene and *p*-xylene are located at $d = 1.4$ Å and $d = 0.6$ Å, respectively. The initial configurations for the trajectories were taken from the CRCD simulations of the transition state presented in paper I.[19] In those simulations, a period of 10 ps passed between two configurations that were used to start a trajectory. The velocity component $\dot{d}(0)$ along the reaction coordinate was assigned from a flux-weighted distribution. There is no need to consider a distortion factor for the CRCD simulations, since only distance constraints are used.[30]

The simulations were performed with a flexible zeolite framework, because the energy transfer from the guest molecule to the zeolite framework may be important in this case. However, a fixed framework had been used in the simulations for the reaction coordinate. When simulations of the transition state with a flexible framework are combined with a reaction coordinate for a fixed framework, the transition state is not identical with one point of the reaction coordinate. Nevertheless, the combination is possible in this case, because we were able to show in paper I[19] that the influence of the framework flexibility on the potential of mean force is negligible.

The trajectories were integrated for 40 ps in both directions of time. Thus, 200 half-trajectories were generated for every temperature. The Verlet algorithm was applied with a time step of 1 ps. The cubic simulation box with the cell parameter $a = 24.85$ Å[25] contains one unit cell of zeolite NaY. The simulations were performed at constant energy with periodic boundary conditions. Results were determined for benzene at 200, 300, 400, 500, and 700 K, and for *p*-xylene at 200, 300, 400, and 500 K.

V. Results of the MD Simulations

A. Transmission Coefficient. The normalized reactive-flux correlation functions $\kappa(t)$ for the transition-state planes of benzene and *p*-xylene at $d = 1.4$ Å and $d = 0.6$ Å, respectively, are depicted in Figure 1. A plateau is obtained for all the temperatures investigated in this work. For both molecules, the height of the plateau of the normalized reactive flux increases with increasing temperature. The transmission coefficients determined from the plateaus are listed in Table 1. The transmission coefficient for *p*-xylene is slightly higher than that for benzene at the same temperature. Nevertheless, both transmission coefficients are relatively small, and therefore the consideration of dynamical corrections in the calculation of the diffusion coefficient will be necessary.

Since there is a local minimum of the potential of mean force in the window,[19] the benzene molecule has to pass over a double barrier to get into the new supercage. The trajectories, which are started near one of the two barrier maxima, may be trapped in the region of the window adsorption site without leaving the vicinity of the transition state on the time scale of the simulations. The fraction $\beta(t)$ of half-trajectories where the center of mass of benzene is located within the range from $d = -1.4$ Å to $d = 1.4$ Å is displayed in Figure 2a. At $t = 0$ ps, $\beta(t)$ starts at 0.5, because each trajectory gets into this range in one direction. At 200 K, $\beta(t)$ contains a plateau, whereas at least one part of the benzene molecules leave the window adsorption site on the time scale of the simulations at higher temperatures. In contrast, *p*-xylene leaves the window region during the simulations even at 200 K, as can be anticipated from Figure 2b, where the fraction $\beta(t)$ of *p*-xylene molecules within the range from $d = -0.6$ Å to $d = 0.6$ Å is displayed.

The transmission coefficient κ for *p*-xylene may be applied to cage-to-cage jumps without further investigations, but the plateau of $\kappa(t)$ for benzene may not automatically be linked to cage-to-cage migration, because the trajectories that are still in the window region cannot be assigned to either supercage and may still change the value of the reactive flux for cage-to-cage migration. However, the determination of the transmission coefficient from the reactive-flux correlation function does not depend on an assignation of each individual molecule to one of two stable states. The correct results are already obtained when the changes in $\kappa(t)$ due to the molecules that have not finally settled in one of the two sides so far can be expected to cancel out.

Depending on the sign of $\dot{d}(0)$, the contribution of a trajectory to the transmission coefficient in eq 4 is either positive or negative. Therefore, it is suitable to display the half-trajectories where benzene is located within the range from $d = -1.4$ Å to $d = 1.4$ Å for positive and negative values of $\dot{d}(0)$ separately. In Figure 3, the functions $\beta_+(t)$ and $\beta_-(t)$ are presented for benzene at 200 and 500 K. At 200 K, the influence of the sign of $\dot{d}(0)$ has ceased after a few picoseconds. It may be assumed that a vast majority of the initial configurations lead to vibrational motion where the sign of $\dot{d}(0)$ is only connected with the phase of the vibration. At 500 K, there remains a difference between $\beta_+(t)$ and $\beta_-(t)$, because the number of trajectories where the starting point is connected to translational movements increases. This effect can explain the increase of the transmission coefficient with increasing temperature.

When $\beta_+(t)$ and $\beta_-(t)$ have become practically identical, the transmission coefficient will remain the same if the molecule leaves the window adsorption site with the same probability in both directions, regardless of the sign of $\dot{d}(0)$. This should be true after at most a few vibrations at the window adsorption site. Therefore, the transmission coefficient for cage-to-cage migration of benzene at low temperatures may be obtained from the plateau of $\kappa(t)$, although the migration out of the window region is a rare event on the time scale of the simulations. At higher temperatures, $\beta_+(t)$ and $\beta_-(t)$ agree no more, but the plateau value of $\kappa(t)$ may be used, because the benzene molecules leave the transition-state region. Thus, the transmission coefficient for cage-to-cage migration of benzene in zeolite NaY could be obtained from the simulations despite the occurrence of a double barrier. As a result, the hopping model need not take into account the window adsorption site explicitly.

B. Absorbing-Boundary Factor. A coordinate r_{WIN} that is defined analogously to the reaction coordinate d is used to define the absorbing boundaries in all of the windows that surround the two-supercage region. The absorbing-boundary functions $\chi(t)$ for the absorbing boundaries of benzene and

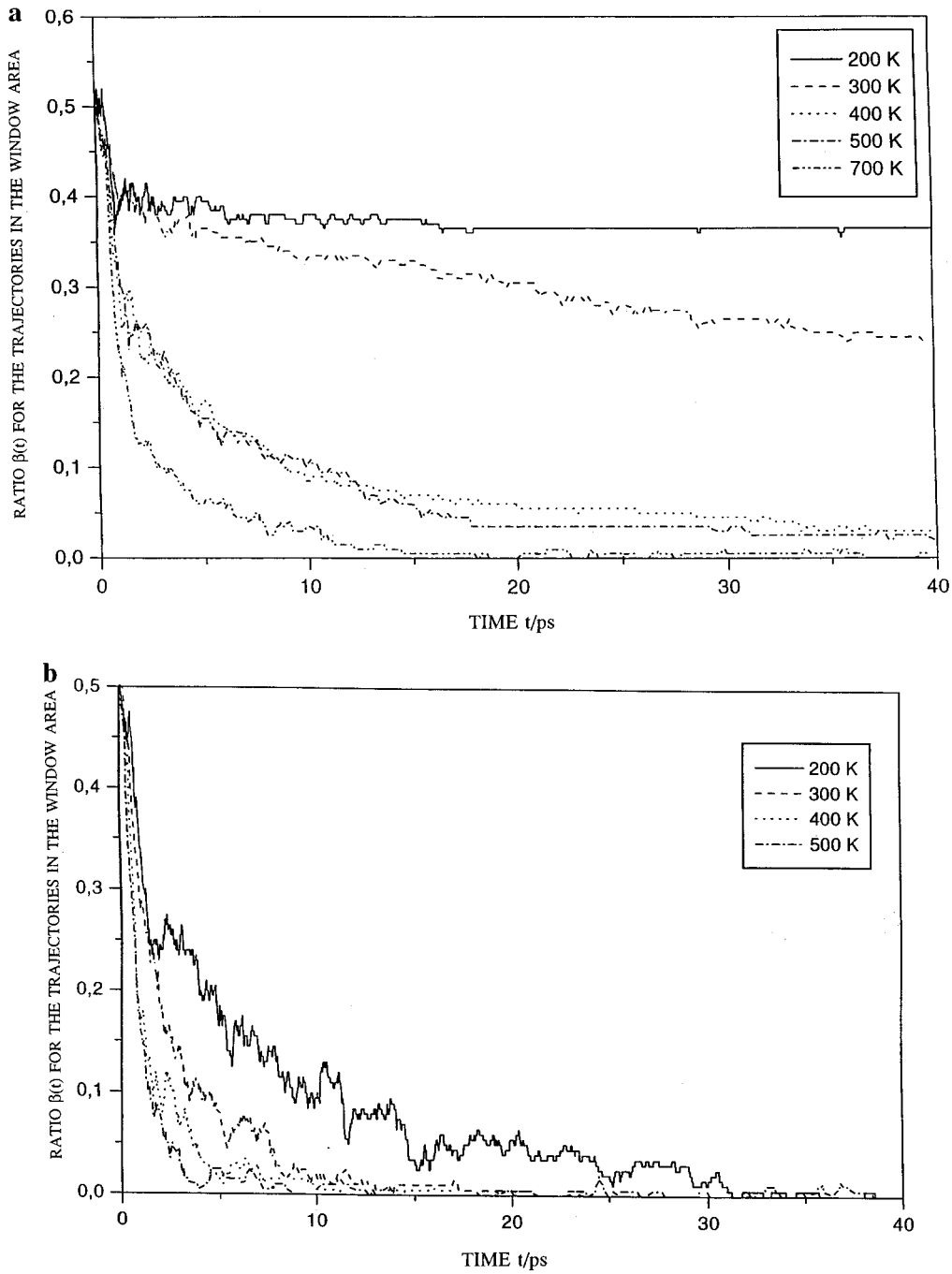

Figure 2. Part $\beta(t)$ of half-trajectories where the center of mass of the guest molecule is located between the transition-state plane and its mirror image at $-d$. The results for benzene with $d = 1.4$ Å (a) and for *p*-xylene with $d = 0.6$ Å (b) are depicted for different temperatures.

p-xylene at $r_{WIN} = -1.4$ Å and $r_{WIN} = 0.6$ Å (see paper I), respectively, are displayed in Figure 4. For both molecules, only a few of the trajectories reach the absorbing boundary at temperatures up to 500 K. At 200 and 300 K, practically all cage-to-cage jumps involve neighboring supercages only. Nevertheless, the results at higher temperatures show that the consideration of trajectories with several barrier passages in the determination of diffusion coefficients of aromatic molecules in zeolite NaY by a hopping model is appropriate.

The absorbing-boundary function $\chi(t)$ for *p*-xylene at 500 K can be well approximated by a straight line in the "plateau" region (see Figure 4b), and the determination of the absorbing-boundary factor χ is therefore possible. On the contrary, the time scale of 40 ps is not sufficient to decide if the absorbing-boundary function $\chi(t)$ for benzene at 700 K allows the determination of an absorbing-boundary factor. Therefore, the simulations at this temperature were prolonged to 100 ps. The absorbing-boundary function $\chi(t)$ for benzene at 700 K during this prolonged period is depicted in Figure 5. The determination of an absorbing-boundary factor at this temperature does not seem appropriate. Thus, the diffusion process cannot be divided into a sequence of independent jump events. Although a plateau of the transmission coefficient κ was obtained at 700 K, the application of a hopping model to the diffusion process has to be restricted to the temperature range from 200 to 500 K. The absorbing-boundary factors χ determined for benzene and *p*-xylene in this temperature range are listed in Table 2.

C. Window Adsorption Site of Benzene. In paper I,[19] the orientation of the aromatic ring was studied by means of the angle φ between the aromatic ring and the transition-state plane. A high value of φ indicates that the aromatic ring is parallel to the walls, i.e., parallel to the reaction coordinate and perpendicular to the transition-state plane. The individual trajectories allow an investigation into the dependence of angle φ on the kind of trajectory. In Table 3, mean angles $\langle\varphi\rangle$ are listed for trajectories with different numbers n_{WIN} of passages through

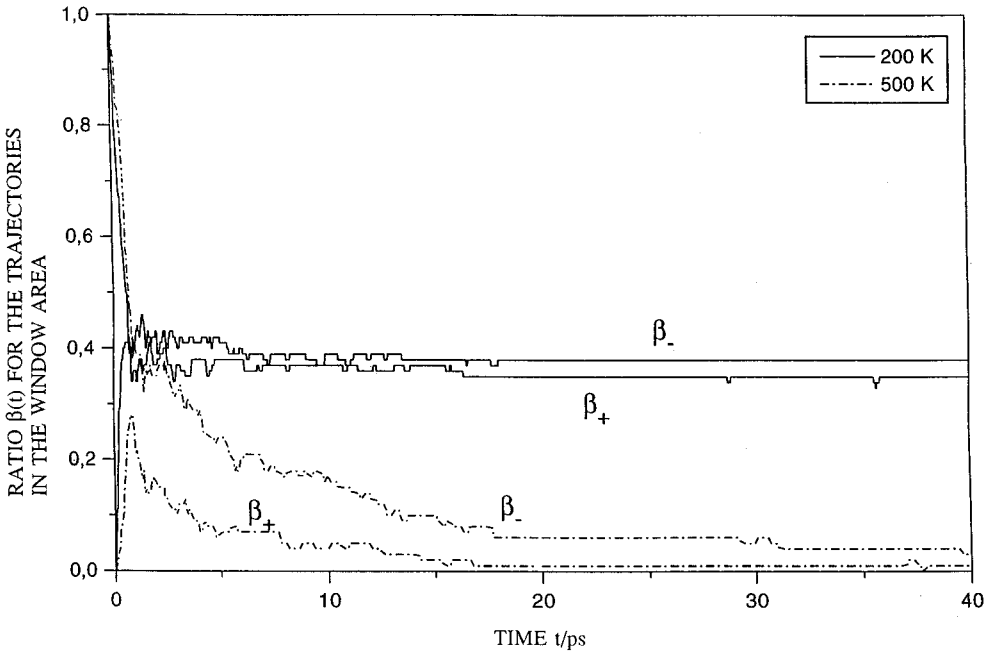

Figure 3. Part $\beta_+(t)$ and $\beta_-(t)$ of half-trajectories with the center of mass of benzene between $d = -1.4$ Åand $d = 1.4$ Å at 200 and 500 K. The indices + and − refer to positive and negative values of the initial velocity $\dot{d}(0)$ along the reaction coordinate.

the window plane. The results have been averaged over the simulations of benzene at 400 and 500 K. Note that two different mean angles are given for the trajectories that pass through the window plane twice, because the starting configuration may be located either near the barrier maximum where the direction of the trajectory is reversed or near the other maximum.

The highest result for the mean angle $\langle\varphi\rangle$ is observed for trajectories that return to the original supercage before they pass through the window plane ($n_{WIN} = 0$). In these trajectories, the aromatic ring remains near the walls. The mean angle $\langle\varphi\rangle$ for trajectories that pass through the window plane at least three times is relatively small, because the typical orientation of molecules that perform vibrations at the window adsorption site is parallel to the window plane. In trajectories that pass through the window plane twice, benzene is set into rotations. Whereas the aromatic ring is oriented rather parallel to the walls during the passage of the first barrier, it is oriented rather perpendicular to the wall during the attempted passage of the second barrier.

Trajectories with $n_{WIN} = 1$ pass over the double barrier without significant changes in the direction of the translational motion. Nevertheless, the mean angle $\langle\varphi\rangle$ decreases from 50.5° to 30.1° during the migration of the molecule from the starting configurations at $d = 1.4$ Å to the window plane at $d = 0$ Å. The passage through the region of the window adsorption site is therefore always connected with a temporary change in the angular orientation of the molecule.

At low temperatures, benzene molecules often remain at the window adsorption site within the time scale of the simulations once they have started to vibrate at this adsorption site. A Fourier transformation of the movements along the reaction coordinate was performed for the 72 half-trajectories that remained at the window adsorption site in the simulations at 200 K. The power spectrum is depicted in Figure 6. The vibrational frequency of benzene at the window adsorption site is around $\tilde{\nu} \approx 23$ cm^{-1}. The movements along the reaction coordinate may be described by a single typical vibration.

There is no such vibrational frequency for *p*-xylene. However, movements of *p*-xylene along the reaction coordinate are only possible in certain angular orientations, and the molecule is hindered from leaving the vicinity of the window plane in others. Collisions with the walls occur, inducing recrossings of the transition-state plane. As a result, the transmission coefficient of *p*-xylene is decreased to a level similar to that of benzene, although there is no stable adsorption site in the window for *p*-xylene.

D. Occupation of Adsorption Sites after the Jump Event. The ratio n_1/n_2 of molecules at the adsorption sites near 4 Å to those at the adsorption site near 9 Å at the end of the 40 ps simulations is listed in Table 4. The ratio is larger than 3, which would result simply from the different number of adsorption sites that contribute to the two minima. Thus, the termination of the jump event at the adsorption sites that are nearer to the central transition state is preferred for both molecules. Very high ratios n_1/n_2 are obtained for *p*-xylene, particularly at low temperatures. The diffusion for *p*-xylene is a succession of jumps between neighboring adsorption sites, and the treatment of the supercage as a joint minimum may not be adequate from these results.

VI. Diffusion Coefficient from the Hopping Model

A. Diffusion Coefficient and Activation Energy. The dynamical corrections for the diffusion of benzene and *p*-xylene in zeolite NaY are listed in Table 5. The probability γ of the continuation of the jump event is small at all temperatures, and accordingly the mean number n_{BP} of barrier passages per jump event is only slightly larger than 1. The typical jump event therefore consists of a jump from one supercage to the next (jumps within the same supercage do not count as jump events). However, the transmission coefficient κ (the local transmission coefficient κ' is nearly identical with κ due to the low value of γ) induces considerable deviations of the dynamically corrected results from the transition-state theory values. These deviations consist of a multiplicative factor given by the product $\kappa' n_{BP}$. The consideration of dynamical corrections therefore decreases the diffusion coefficient of *p*-xylene by a factor of 2−4 and that of benzene by up to an order of magnitude.

The calculated diffusion coefficients D of benzene and *p*-xylene are listed in Table 6. At all temperatures, the diffusion coefficient of *p*-xylene is larger than that for benzene. The diffusion coefficients strongly increase with increasing temperature. The temperature dependence of the diffusion is described

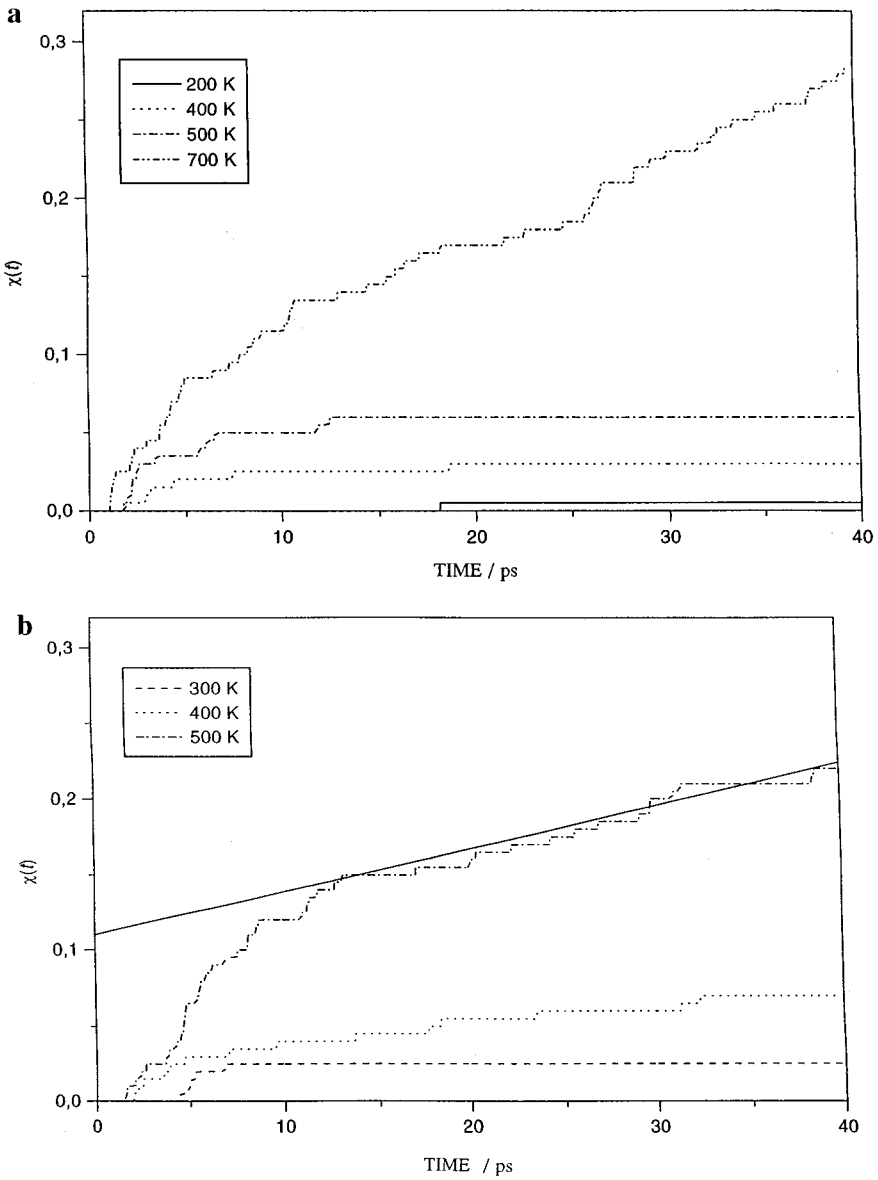

Figure 4. Absorbing-boundary function $\chi(t)$ for the absorbing boundaries of benzene at $r_{WIN} = -1.4$ Å (a) and *p*-xylene at $r_{WIN} = 0.6$ Å (b) at different temperatures.

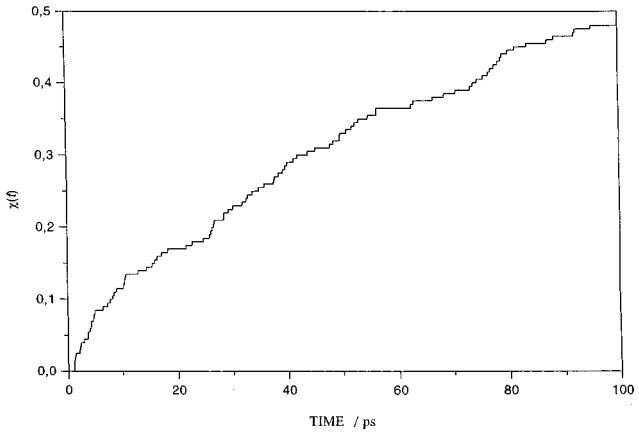

Figure 5. Absorbing-boundary function $\chi(t)$ for benzene in zeolite NaY at 700 K (simulations prolonged to 100 ps).

by the Arrhenius activation energy E_A:

$$\frac{\partial \ln D}{\partial(1/T)} = \frac{E_A}{R} \tag{10}$$

The Arrhenius plots for benzene and *p*-xylene are displayed in Figure 7a,b, respectively. The activation energies are $E_A = 49.5 \pm 4.1$ kJ/mol for benzene and 24.6 ± 4.2 for *p*-xylene. The contributions of the dynamical corrections to the activation energy, determined from an investigation of the temperature

TABLE 2: Absorbing-Boundary Factors for Benzene and *p*-Xylene in Zeolite NaY

	absorbing-boundary factor χ	
temperature T [K]	benzene	*p*-xylene
200	0.0	0.0
300	0.0	0.03
400	0.03	0.03
500	0.05	0.11

TABLE 3: Interrelation between Angle φ and Number of Passages through Window Plane for Benzene[a]

number n_{WIN} of passages through window plane	mean angle $\langle\varphi\rangle$	standard deviation $\sigma(\varphi)$	number of trajectories
0	71.6	13.6	64
1	50.5	18.8	40
2	60.8	19.3	11
2	30.1	13.2	8
≥3	37.5	23.9	77

[a] From the results of the simulations at 400 and 500 K.

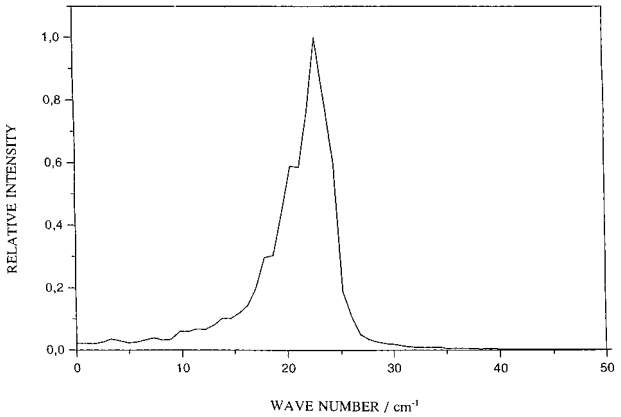

Figure 6. Fourier transformation of the movements along the reaction coordinate d for benzene molecules at the window adsorption site. The results were determined from the half-trajectories that remained at the window adsorption site in the simulations at 200 K.

TABLE 4: Ratio n_1/n_2 of Molecules at Different Adsorption Sites[a,b]

ratio n_1/n_2 temperature T [K]	benzene	*p*-xylene
200	16	∞[c]
300	10	48
400	10	10
500	5.4	6.2
700	3.5	*d*

[a] Ratio of molecules at the three adsorption sites near $d = 4$ Å to molecules at the adsorption site near $d = 9$ Å. [b] After 40 ps (at the end of the simulations). [c] No molecules at $d = 9$ Å. [d] No simulations at this temperature.

TABLE 5: Dynamical Corrections for the Diffusion of Benzene and *p*-Xylene in Zeolite NaY

	benzene			*p*-xylene		
T [K]	γ[a]	n_{BP}[b]	$\kappa' n_{BP}$[c]	γ[a]	n_{BP}[b]	$\kappa' n_{BP}$[c]
200	0.00	1	0.08	0.00	1	0.24
300	0.00	1	0.20	0.01	1.01	0.28
400	0.01	1.01	0.18	0.02	1.02	0.54
500	0.02	1.02	0.30	0.07	1.07	0.52

[a] Probability γ for the continuation of the jump event. [b] Mean number n_{BP} of barrier passages per jump event. [c] Factor $\kappa' n_{BP}$ representing the dynamical corrections.

TABLE 6: Calculated Diffusion Coefficients for Benzene and *p*-Xylene in Zeolite NaY

	diffusion coefficient D [cm^2 s^{-1}]	
temperature T [K]	benzene	*p*-xylene
200	7.5×10^{-15}	1.1×10^{-9}
300	2.3×10^{-10}	1.5×10^{-7}
400	1.5×10^{-8}	1.9×10^{-6}
500	5.4×10^{-7}	7.4×10^{-6}

dependence of $\kappa' n_{BP}$, are 3.3 ± 0.8 and 2.4 ± 0.8 kJ/mol for benzene and *p*-xylene, respectively.

B. Discussion. Whereas the calculated diffusion coefficient for benzene is smaller than the one for *p*-xylene, the experiments yield a larger diffusion coefficient for benzene. Nevertheless, there is good agreement between the calculated and the experimental results for *p*-xylene. The calculated activation energy for *p*-xylene is at the lower end of the range of 25−31 kJ/mol determined experimentally[1,2,7,10,11] for *p*-xylene in zeolites NaX and NaY at lower loadings. Moreover, the diffusion coefficient $D = 1.9 \times 10^{-6}$ cm^2/s at 400 K differs only by a factor of 4 from the diffusion coefficient of 5×10^{-7} cm^2/s that Germanus et al.[1] determined by PFG-NMR for *p*-xylene in zeolite NaX at the same temperature. The difference between the two results could possibly partly result from the differences in the loading. Moreover, if the four adsorption sites within the supercage were considered explicitly in the hopping model, the initial occupation of adsorption sites near the window of entry would induce a preference for the next jump to occur in the reverse direction, reducing the diffusion coefficient. Therefore, the agreement between the MD simulations and PFG-NMR is possibly even better than it is expressed by the similarity of the diffusion coefficients.

TABLE 7: Force Field Parameters for Interactions between Benzene Molecules[a]

force centers	ϵ [kJ mol^{-1}]	σ [Å]
C−C	0.398	3.467
C−H	0.146	3.189
H−H	0.0534	2.910

[a] Taken from ref 21.

The calculated activation energy for benzene, however, is larger than most of the experimental results for this system. Nevertheless, it is in very good agreement with the results of the Mone Carlo approach of Auerbach et al.,[15] since their activation energy of 41 kJ/mol is reduced by neglecting both the dynamical corrections and the temperature dependence of the activation barrier that became apparent in the potential of mean force presented in ref 19. Furthermore, the activation energy is in good accordance with the activation energy of 46 kJ/mol determined by Forni and Viscardi.[9] In the temperature range investigated in this work, the calculated diffusion coefficients are significantly smaller than those determined by Germanus et al.,[1] although both approaches determine the self-diffusion coefficient on a microscopic level. For temperatures around 400 K, better agreement is obtained when the calculated diffusion coefficients are compared with the results of Goddard and co-workers.[2,10,11] Due to the differences in the activation energy, this has, however, to be seen as coincidental.

Garcia and Weisz[13] suggested that the discrepancy between the PFG-NMR results and those of the macroscopic methods are due to the exclusive measurement of a specific activated state of diffusing molecules in the PFG-NMR experiments. However, the low value of the absorbing-boundary factor χ in the simulations implies that most of the jump events are very short at temperatures up to 500 K. There are no indications for the occurrence of a specific activated state that is connected with long-range diffusion processes. Thus, the discrepancy between the different results for the diffusion coefficient of aromatic compounds in zeolites NaX and NaY further awaits explanation.

We additionally performed conventional MD simulations of benzene in zeolite NaY at very high temperatures to confirm that the high activation energy is indeed typical for the model system used in the simulations. Simulations with 64 benzene molecules without interactions between the guest molecules were performed at 800, 1000, and 1200 K. Furthermore, simulations with two benzene molecules per supercage in the unit cell were carried out at 800, 1000, 1200, and 1400 K. The parameters (listed in Table 7) for the interactions between different benzene molecules are based on the force field of Demontis et al.[21] The simulations were performed with a fixed zeolite framework for periods between 350 and 1200 ps. Diffusion coefficients from these simulations were obtained from the Einstein relation

$$\langle |r_i(t) - r_i(0)|^2 \rangle = 6Dt \qquad (11)$$

In Figure 8, the results of the conventional MD simulations are compared with the results of the hopping model. The conventional MD simulations result in an activation energy of ca. 40 kJ/mol at both loadings. All the results at infinite dilution

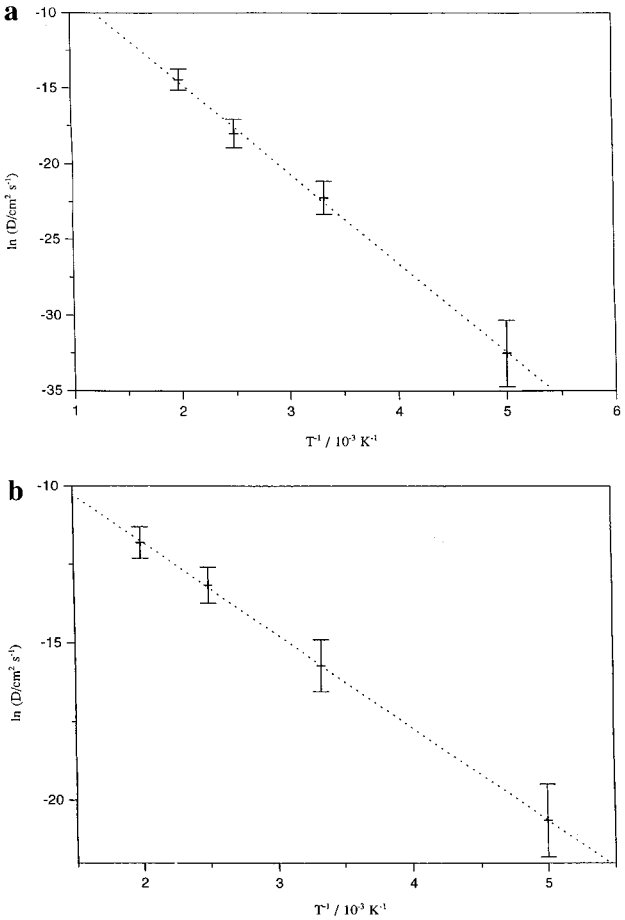

Figure 7. Arrhenius plots for the diffusion coefficients of benzene (a) and *p*-xylene (b) in zeolite NaY.

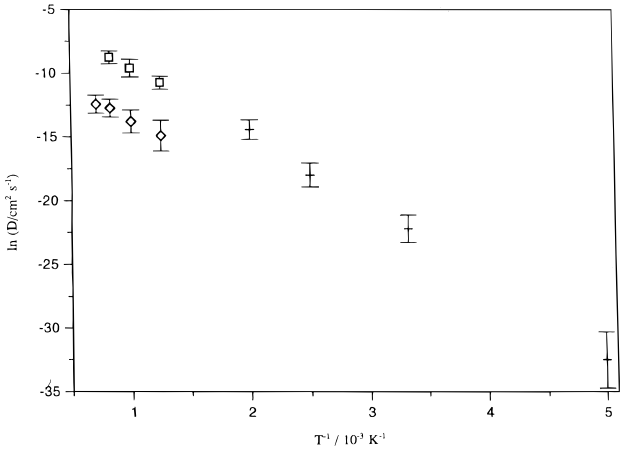

Figure 8. Arrhenius plot for the diffusion coefficient of benzene in zeolite NaY. The results of the conventional MD simulations at infinite dilution (□) and a loading of 2 molecules per supercage (◇) are compared to the results determined from the hopping model (+).

agree well, confirming the applicability of the hopping model. The difference between the activation energy of the hopping model and that of the high-temperature simulations may be due to a slight temperature dependence of the activation energy. At a loading of two benzene molecules per supercage, the diffusion coefficient is significantly smaller, but the activation energy of the diffusion remains unchanged. Therefore, the high activation energy is not the result of a dependence of the activation energy on the loading.

We presume that the high activation energy for the model system of benzene in zeolite NaY results from the simplifications in the model representation of the zeolite. Some important approximations were introduced for the extraframework cation positions of sodium. The shift of the sodium ions on the $S_{I'}$ position to position S_I should not influence the behavior of benzene significantly, because both positions are close to each other and benzene cannot enter the vicinity of either of them. As a result, Auerbach et al., who used the $S_{I'}$ position instead of position S_I, determined a very similar activation energy. Position S_{III} is inside the supercage and can be reached by the aromatic molecules. Position S_{III} seems to be occupied only scarcely in zeolite NaY with relatively low content of aluminum, but it should be populated significantly in zeolite NaX. Moreover, there could be a certain amount of dislocated cations in some experimental samples of zeolite NaY even with a high Si/Al ratio. Since the interactions between sodium and the framework oxygens are modeled by bonded potentials, even dynamic processes where sodium temporarily leaves the vicinity of the minimum in position S_{II}—even without reaching position S_{III}—may be suppressed by the model.

Differences in the distribution of sodium on the cation positions could also accout for the differences between the activation energies determined in different experimental investigations. The *p*-xylene molecule is larger than benzene, and an orientation where the energy in the transition state is decreased by favorable interactions with shifted cations may be impossible for *p*-xylene. This would explain why a similar difference between calculated and experimental activation energy does not occur for *p*-xylene. The possibility of an involvement of sodium on position S_{III} or of far-reaching dynamic movements of sodium on position S_{II} in the diffusion of benzene should be the topic of further investigations.

VII. Conclusions

The diffusion process of benzene and *p*-xylene in zeolite NaY was investigated by means of MD simulations of individual trajectories started in the transition state for cage-to-cage diffusion. The transmission coefficient for both molecules is rather small, particularly at low temperatures. The smaller transmission coefficient is observed for benzene where the result is influenced by the occurrence of a window adsorption site. It was shown that the transmission coefficient for benzene is characteristic for cage-to-cage jumps despite the existence of the window adsorption site. Thus, it is possible to describe the diffusion process of benzene in zeolite NaY by a hopping model that does not consider the window adsorption site explicitly.

During the passage of the window region, a partial reorientation of the benzene ring with respect to the zeolite walls occurs, even in trajectories that pass through the window region directly. The orientation of the benzene ring in the transition state significantly affects the behavior of the trajectory in the vicinity of the window adsorption site.

The absorbing-boundary factor that describes the tendency of the guest molecule to pass over several barriers within one jump event is small at temperatures up to 500 K for both aromatic molecules. In the simulations of benzene at 700 K, however, it is impossible to determine an adsorbing-boundary factor and the diffusion cannot be divided into different jump events.

Diffusion coefficients were calculated for temperatures up to 500 K by the hopping model described in ref 18. The results for *p*-xylene are in good agreement with experimental results. The calculated activation energy for benzene is in accordance with the simulation results of Auerbach et al.,[15] but it is at the upper end of the range of experimentally determined activation energies. Furthermore, the diffusion coefficient is smaller than expected from the PFG-NMR experiments of Germanus et al.[1] We presume that the high activation energy in the simulation studies results from the positions of the sodium ions. Sodium

on position S_{III} inside the supercage may possibly be involved in the diffusion process of benzene in zeolite NaY, although Fitch et al.[25] did not observe sodium ions on this position in their X-ray investigation of zeolite NaY. Alternatively, dynamic processes where sodium temporarily leaves position S_{II} may induce a decrease of the activation energy of benzene in zeolites NaX and NaY. These differences in the sodium positions could also account for the wide range of experimental activation energies. The importance (and the details) of this possible involvement of sodium ions in the diffusion of benzene should be the topic of further investigations.

The successful application of transition-state theory with dynamical corrections to the diffusion of guest molecules in zeolites has shown that the hopping model for the calculation of diffusion coefficients from jump rates can appropriately describe diffusion processes in zeolites. In the future, this hopping model may be applied to the diffusion of other guest molecules and of extraframework cations. Moreover, the hopping model can easily be modified to the geometry of other zeolites.

Acknowledgment. We thank the Fonds der Chemischen Industrie, Frankfurt, for financial support of this work.

References and Notes

(1) Germanus, A.; Kärger, J.; Pfeifer, H.; Samulevič, N. N.; Zd'anov, S. P. *Zeolites* **1985**, *5*, 91.
(2) Eic, M.; Goddard, M.; Ruthven, D. M. *Zeolites* **1988**, *8*, 327.
(3) Boddenberg, B.; Burmeister, R. *Zeolites* **1988**, *8*, 488.
(4) Shen, D.; Rees, L. V. C. *Zeolites* **1991**, *11*, 666.
(5) Lechert, H.; Wittern, K. P. *Ber. Bunsen-Ges. Phys. Chem.* **1979**, *83*, 596.
(6) Bull, L. M.; Henson, N. J.; Cheetham, A. K.; Newsam, J. M.; Heyes, S. J. *J. Phys. Chem.* **1993**, *97*, 11776.
(7) Sousa Gonçalves, J. A.; Portsmouth, R. L.; Alexander, P.; Gladden, L. F. *J. Phys. Chem.* **1995**, *99*, 3317.
(8) Burmeister, R.; Schwarz, H.; Boddenberg, B. *Ber. Bunsen-Ges. Phys. Chem.* **1989**, *93*, 1309.
(9) Forni, L.; Viscardi, C. F. *J. Catal.* **1986**, *97*, 480.
(10) Goddard, M.; Ruthven, D. M. *Zeolites* **1986**, *6*, 283.
(11) Goddard, M.; Ruthven, D. M. *Zeolites* **1986**, *6*, 445.
(12) Kärger, J.; Ruthven, D. M. *Diffusion in Zeolites and Other Microporous Solids*; John Wiley: New York, 1992.
(13) Garcia, S. F.; Weisz, P. B. *J. Catal.* **1990**, *121*, 294.
(14) Joly, G.; Tessa, N. *Bull. Soc. Chim. Fr.* **1993**, *130*, 223.
(15) Auerbach, S. M.; Henson, N. J.; Cheetham, A. K.; Metiu, H. I. *J. Phys. Chem.* **1995**, *99*, 10600.
(16) June, R. L.; Bell, A. T.; Theodorou, D. N. *J. Phys. Chem.* **1991**, *95*, 8866.
(17) Mosell, T.; Schrimpf, G.; Hahn, C.; Brickmann, J. *J. Phys. Chem.* **1996**, *100*, 4571.
(18) Mosell, T.; Schrimpf, G.; Brickmann, J. *J. Phys. Chem.* **1996**, *100*, 4582.
(19) Mosell, T.; Schrimpf, G.; Brickmann, J. *J. Phys. Chem.* **1997**, *101*, 9476.
(20) Carter, E. A.; Ciccotti, G.; Hynes, J. T.; Kapral, R. *Chem. Phys. Lett.* **1989**, *156*, 472.
(21) Demontis, P.; Yahonath, S.; Klein, M. L. *J. Phys. Chem.* **1989**, *93*, 5016.
(22) Bezus, A. G.; Kiselev, A. V.; Lopatkin, A. A.; Du, P. Q. *J. Chem. Soc., Faraday Trans. 2* **1978**, *74*, 367.
(23) Dewar, M. J. S.; Zoebisch, E. G.; Healy, E. F.; Stewart, J. J. P. *J. Am. Chem. Soc.* **1985**, *107*, 3902.
(24) Schrimpf, G.; Schlenkrich, M.; Brickmann, J.; Bopp, P. *J. Phys. Chem.* **1992**, *96*, 7404.
(25) Fitch, A. N.; Jobic, H.; Renouprez, A. *J. Phys. Chem.* **1986**, *90*, 1311.
(26) Wigner, E. *Trans. Faraday Soc.* **1938**, *34*, 29.
(27) Eyring, H. *J. Chem. Phys.* **1935**, *3*, 107.
(28) Chandler, D. *J. Chem. Phys.* **1978**, *68*, 2959.
(29) Voter, A. F.; Doll, J. D. *J. Chem. Phys.* **1985**, *82*, 80.
(30) Ciccotti, G.; Ferrario, M.; Hynes, J. T.; Kapral, R. *J. Chem. Phys.* **1990**, *93*, 7137.
(31) Keirstaed, W. P.; Wilson, K. R.; Hynes, J. T. *J. Chem. Phys.* **1991**, *95*, 5256.
(32) Berne, B. J.; Borkovec, M.; Straub, J. E. *J. Phys. Chem.* **1988**, *92*, 3711.
(33) Manning, J. R. *Diffusion Kinetics for Atoms in Crystals*; van Nostrand: Princeton, 1968.